

# Recent Belle Results on $CP$ -Violation

## Representing the Belle Collaboration

P. Pakhlov\*

*ITEP, Moscow, Russia*

23rd May 2002

We present a measurement of the Standard Model  $CP$ -violation parameter  $\sin 2\phi_1$  based on  $10.5 \text{ fb}^{-1}$  data sample collected at the  $\Upsilon(4S)$  resonance with the Belle detector at the KEKB asymmetric  $e^+e^-$  collider. One  $B$  meson is reconstructed in the  $J/\psi K_S$ ,  $\psi(2S)K_S$ ,  $\chi_{c1}K_S$ ,  $J/\psi\pi^0$  or  $J/\psi K_L$   $CP$ -eigenstate decay channel while the flavor of the accompanying  $B$  is identified by the charge of the particles from its decay. From the asymmetry in the distribution of the time interval between the two  $B$ -meson decay points, we determined  $\sin 2\phi_1 = 0.58^{+0.32}_{-0.34}(\text{stat})^{+0.09}_{-0.10}(\text{syst})$ .

## 1 Introduction

The  $CP$ -violation remains one of the intriguing features of the high energy physics since its experimental discovery in neutral  $K$ -system in 1964 [1]. It took almost a decade for a suitable explanation of this effect introducing the Cabibbo-Kobayashi-Maskawa (CKM) quark mixing matrix with an irreducible complex phase as a single source of  $CP$  violation [2]. So far the only information about this phase comes from the measured value of the  $CP$  violating parameter  $\epsilon$  in  $K^0$  system. This measurement is accommodated in the CKM approach, but it can not test the theory where the complex phase remains a free parameter.  $B$  physics provides a wide variety of independent  $CP$  asymmetry measurements related to different sectors of the CKM matrix and becomes a basis for testing the CKM mechanism.

On the other hand  $B$  physics is a powerful tool for measuring the fundamental parameters of the Standard Model. Most information about the elements of the CKM matrix was extracted from  $B$  decays. However, the interpretation of the experimental measurements suffers from the QCD uncertainties. Actually, only few measurements in  $B$  decays can be used for model independent constraints on the CKM matrix elements. The measurement of time-dependent  $CP$  asymmetry in the decay  $B^0 \rightarrow (c\bar{c})K^0$  provides for the exact calculation of  $\sin 2\phi_1$ , where  $\phi_1$  is one of the angles in the CKM Unitarity Triangle, defined as  $\phi_1 \equiv \pi - \arg(-V_{tb}^*V_{td})/(-V_{cb}^*V_{cd})$ . In the  $\phi_1$  calculation, ambiguities due to strong interactions and direct  $CP$ -violation effects are expected to be very small.

Finally,  $B$  physics is believed to be one of the most promising fields for a new physics search at the existing accelerators. The large  $b$ -quark mass, the standard decays suppression by  $|V_{cb}|$  and  $|V_{ub}|$  matrix elements and significant contribution from the loop and box diagrams, to which new particles, even very heavy, can contribute, make  $B$  physics very attractive from this point of view. Again,  $CP$  violation pattern in  $B$  decays could be the best probe for the physics beyond the Standard Model because of clear and reliable theoretical predictions in the Standard Model framework on the one hand and because  $CP$  violation tests the box and loop diagrams in  $B$  decay

---

\*E-mail: pakhlov@iris1.itep.ru

on the other. Possible scenarios of  $CP$  violation beyond the Standard Model are widely discussed in literature (see *eg.* [3]).

The Standard Model predicts large  $CP$  violating effects in  $B$  decays due to the interference between the direct  $B^0 \rightarrow f_{CP}$  and mixing induced  $B^0 \rightarrow \bar{B}^0 \rightarrow f_{CP}$  decay amplitudes, where  $f_{CP}$  is a  $CP$  eigenstate to which both  $B^0$  and  $\bar{B}^0$  can decay. In  $\Upsilon(4S)$  decays  $B$  pairs are produced in P-wave and because of Bose statistics remain in a coherent  $B^0\bar{B}^0$  state until one of them decays. If it decays to a specific flavor final state  $f_{tag}$  at time  $t_{tag}$ , the accompanying  $B$  meson is projected onto the orthogonal state at that time. The latter  $B$  meson then propagates in time and can decay to  $f_{CP}$ . These speculations remain valid in case if the first  $B$  decays into the  $CP$  final state before the second  $B$  decays into the tagging state, though the sign of the observed asymmetry inverted. Thus the time-integrated asymmetry vanishes. For  $f_{CP} = (c\bar{c})K^0$  the time-dependent  $CP$  violating asymmetry takes the form:

$$A(\Delta t) \equiv \frac{\Gamma(\bar{B}^0 \rightarrow f_{CP}) - \Gamma(B^0 \rightarrow f_{CP})}{\Gamma(\bar{B}^0 \rightarrow f_{CP}) + \Gamma(B^0 \rightarrow f_{CP})} = -\xi_{CP} \sin 2\phi_1 \sin \Delta m \Delta t,$$

where  $\Delta t \equiv t_{CP} - t_{tag}$  is the proper time interval,  $\xi_{CP}$  is the  $CP$  eigenvalue of the final state eigenmode,  $\Delta m$  is the mass difference between  $B$  meson mass eigenstates.

Here we report a measurement of  $\sin 2\phi_1$  using the data sample that corresponds to an integrated luminosity of  $10.5 \text{ fb}^{-1}$  collected with the Belle detector at the KEKB  $e^+e^-$  collider.

## 2 The Belle Detector

The Belle detector [4] is a large solid-angle magnetic spectrometer operating at the asymmetric  $e^+e^-$  collider KEKB [5]. Charged particles are reconstructed in a 50-layer central drift chamber (CDC) and their impact parameters are precisely determined using a three-layer silicon vertex detector (SVD). The transverse momentum resolution is  $\sigma_{p_t}/p_t = 0.0034 \oplus 0.0019p_t$ , and the impact parameter resolution for  $p = 1 \text{ GeV}/c$  tracks at normal incidence is  $\sigma_{IP} = 55 \text{ }\mu\text{m}$ .

The identification of charged tracks is based on the specific ionization measurements in the CDC ( $\sigma_{dE/dx} = 6.9 \%$ ), the time of flight measurements ( $\sigma_t = 95 \text{ ps}$ ) and the response from aerogel Cherenkov counters (ACC), providing  $K/\pi$  separation with an efficiency of  $\sim 85\%$  and a fake rate of  $\sim 10\%$  for all momenta up to  $3.5 \text{ GeV}/c$ .

Photons are reconstructed in electro-magnetic calorimeter (ECL) as showers with an energy larger than  $20 \text{ MeV}$  which are not associated with charged tracks. The energy resolution is  $\sigma_E/E = 0.0066/E \oplus 0.015/E^{1/4} \oplus 0.0118$ , where  $E$  is measured in  $\text{GeV}$ .

Electron identification is based on a combination of  $dE/dx$  measurements, the ACC response and the information about shape, energy deposit and position of the associated ECL shower. The identification efficiency is greater than  $90\%$  while the hadron fake rate is  $\sim 0.3\%$  for  $p > 1 \text{ GeV}/c$ .

Muon identification is provided by 14 layers of  $4.7 \text{ cm}$  thick iron plates interleaved with a system of resistive plate counters (KLM). The efficiency is over  $90\%$  and the hadron fake rate is smaller than  $2\%$  for  $p > 1 \text{ GeV}/c$ .

$K_L$  mesons are detected as KLM hits not associated with charged tracks. If there is an ECL hit associated with a  $K_L$  candidate, its direction is determined from the center of gravity of the ECL shower alone, otherwise from the average position of the KLM hits. The angular resolution of the  $K_L$  direction is estimated to range from  $1.5^\circ$  to  $3^\circ$ .

### 3 Signal selection

We reconstruct  $B^0$  decays to the following  $CP$  eigenstates:  $J/\psi K_S$ ,  $\psi(2S)K_S$ ,  $\chi_{c1}K_S$  for  $\xi_f = -1$  and  $J/\psi\pi^0$ ,  $J/\psi K_L$  for  $\xi_f = +1$  [6].

The  $J/\psi$  and  $\psi(2S)$  are reconstructed via their decays to  $\ell^+\ell^-$  ( $\ell = \mu, e$ ). Fig. 1 shows the dimuon and dielectron invariant mass spectra after the selection of two identified leptons. The  $\psi(2S)$  is also reconstructed in the  $J/\psi\pi^+\pi^-$  decay mode. The  $\chi_{c1}$  is reconstructed via its  $J/\psi\gamma$  decay, and the  $\eta_c$  via its  $K^+K^-\pi^0$  and  $K_S K^- \pi^+$  decays. For the  $J/\psi K_S$  mode we use both  $K_S \rightarrow \pi^+\pi^-$  and  $\pi^0\pi^0$  decays; for other modes we use only  $K_S \rightarrow \pi^+\pi^-$ . For the  $J/\psi\pi^0$  mode, we select  $\gamma\gamma$  pairs with a minimum  $\gamma$  energy of 100 MeV and with an invariant mass within  $\pm 3\sigma$  of the nominal  $\pi^0$  mass.

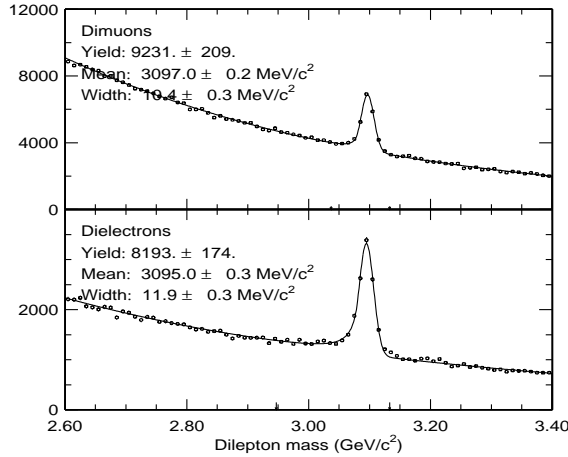


Figure 1. The invariant mass distributions for  $J/\psi \rightarrow \mu^+\mu^-$  (upper) and  $J/\psi \rightarrow e^+e^-$  (lower).

Reconstructed charmonium candidates are then combined with  $K_S$  or  $\pi^0$  to form a  $B^0$  candidate and two variables are used to select the signal: the energy difference  $\Delta E \equiv E_B - \sqrt{s}/2$ , and the beam-constrained mass  $M_{bc} \equiv \sqrt{s/4 - p_B^2}$ , where  $E_B$  and  $p_B$  are the  $B$  candidate's cms energy and momentum. The  $M_{bc}$  plot for all decay modes combined other than  $J/\psi K_L$  is shown in Fig. 2 after the  $\Delta E$  selection varying from  $\pm 25$  MeV to  $\pm 100$  MeV depending on the mode.

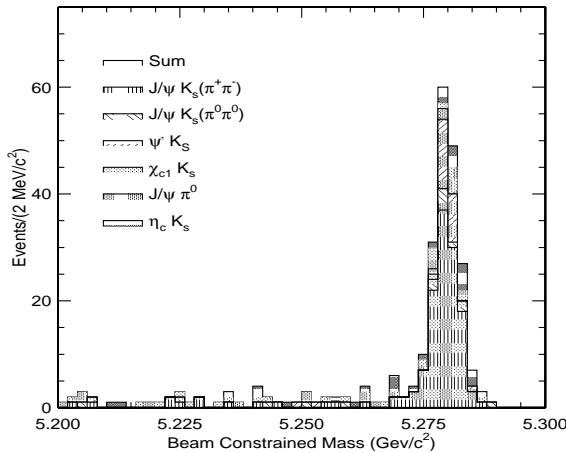


Figure 2. The beam-constrained mass distribution for all decays modes combined (other than  $B^0 \rightarrow J/\psi K_L$ ).

$B^0 \rightarrow J/\psi K_L$  decay candidates are selected by requiring the observed  $K_L$  direction to be within

45° from the direction expected for two-body decay. The background is further suppressed using the likelihood based on the charged track multiplicity, the angle between the  $K_L$  candidate and the nearest charged track, and some other kinematic quantities. In addition, we also remove events with fully reconstructed  $B^0 \rightarrow J/\psi K_S$ ,  $B^+ \rightarrow J/\psi K^+$ ,  $B^0 \rightarrow J/\psi K^{*0}$ ,  $B^+ \rightarrow J/\psi K^{*+}$ . Fig. 3 shows the  $p_B$  distribution for the selected candidates. Here the  $B^0 \rightarrow J/\psi K_L$  signal shows up as a distinct peak near  $p_B \simeq 340$  MeV/c; the background comes mainly from  $B \rightarrow J/\psi K^*$  decays. These decays are understood from the studies of  $B \rightarrow J/\psi K^*$  events where  $K^* \rightarrow K^+ \pi$  or  $K_S \pi$  and well described by the Monte Carlo simulation, which is used to generate the shape shown as the shaded histogram in the figure. There are 131 events in the  $0.2 < p_B^* < 0.45$  MeV/c signal region; the fit finds a total of 77  $J/\psi K_L$  signal events.

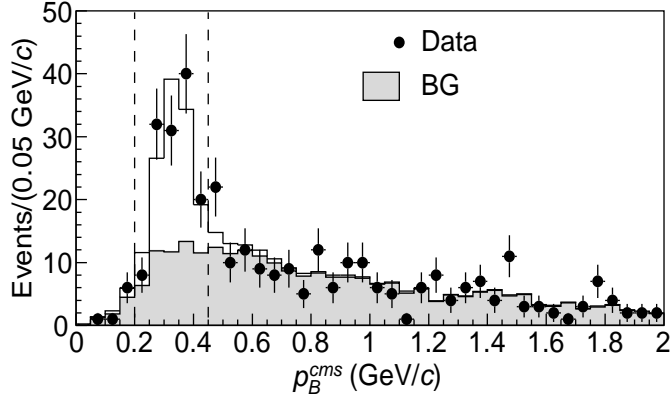


Figure 3. The  $p_B$  distribution with the fit result. The upper solid line is the sum of signal and background; the shaded histogram is the MC-determined background.

The number of signal-region events and the background levels for each mode are summarized in Table 1.

Table 1. The numbers of  $CP$  eigenstate events

| Decay mode                                      | $N_{ev}$ | $N_{bkgd}$ |
|---|----------|------------|
| $J/\psi(\ell^+ \ell^-) K_S(\pi^+ \pi^-)$        | 123      | 3.7        |
| $J/\psi(\ell^+ \ell^-) K_S(\pi^0 \pi^0)$        | 19       | 2.5        |
| $\psi(2S)(\ell^+ \ell^-) K_S(\pi^+ \pi^-)$      | 13       | 0.3        |
| $\psi(2S)(J/\psi \pi^+ \pi^-) K_S(\pi^+ \pi^-)$ | 11       | 0.3        |
| $\chi_{c1}(J/\psi \gamma) K_S$                  | 3        | 0.5        |
| $\eta_c(K^+ K^- \pi^0) K_S(\pi^+ \pi^-)$        | 10       | 2.4        |
| $\eta_c(K_S K^- \pi^+) K_S(\pi^+ \pi^-)$        | 5        | 0.4        |
| $J/\psi(\ell^+ \ell^-) \pi^0$                   | 10       | 0.9        |
| Sub-total                                       | 194      | 11         |
| $J/\psi(\ell^+ \ell^-) K_L$                     | 131      | 54         |

## 4 Flavor tagging

The leptons, kaons and charged pions that are not involved into the  $CP$  final state reconstruction are used for flavor identification of the accompanying  $B$  meson. Several charged track categories are selected to determine the  $b$  flavor by the track charge:

- high momentum leptons from  $b \rightarrow c \ell^- \bar{\nu}$ ,

- medium momentum leptons from  $b \rightarrow c \rightarrow s\ell^+\nu$ ,
- charged kaons from  $b \rightarrow c \rightarrow s$ ,
- high momentum pions from decays of the type  $B^0 \rightarrow D^{(*)-}(\pi^+, \rho^+, \text{etc.})$ ,
- slow pions from  $D^{*-} \rightarrow \bar{D}^0 \pi^-$ .

For each track in one of these categories, we determine using the Monte Carlo simulation the relative probability that it originates from a  $B^0$  or  $\bar{B}^0$  as a function of its charge, momentum in the center of mass frame, particle identification probability as well as other kinematic and event shape quantities. The results from the different track categories are then combined taking into account their possible correlations. Finally the tagging probability is represented in terms of a dilution factor  $r = (1 - 2\omega_l)^2$ , where  $\omega_l$  is the probability of the incorrect flavor tagging.  $r$  is only used to sort data into six intervals with different flavor purity. The fraction of events and the wrong tagging probabilities in each interval are determined directly from the data. For this purpose we use a large sample of exclusively reconstructed and self-tagged  $B^0$  decays into  $D^{*-}\ell^+\nu$ ,  $D^{(*)-}\pi^+$ , and  $D^{(*)-}\rho^+$ . The values of  $\omega_l$  are obtained from the amplitudes of the time-dependent  $B^0\bar{B}^0$  oscillations. The exclusive decays and the tag vertices are reconstructed using the same vertex algorithm that is used to measure  $CP$  asymmetry as discussed below. The  $B^0\bar{B}^0$  oscillation plots are shown in Fig. 4 for the six  $r$  intervals using the  $B^0 \rightarrow D^{*-}\ell^+\nu$  channel only. The curves represent the result of the fit by a function describing the expected mixing behavior depending on  $\omega_l$  as free parameters. Table 2 lists the resulting  $\omega_l$  values together with the fraction of events,  $f_l$ , in each  $r$  interval. The total effective tagging efficiency is  $\sum_l f_l (1 - 2\omega_l)^2 = 0.270_{-0.022}^{+0.021}$  in good agreement with the Monte Carlo result of 0.274.

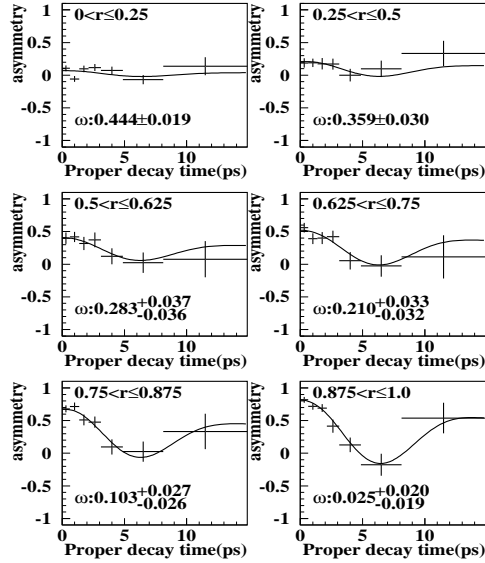


Figure 4. The measured time-dependent  $B^0\bar{B}^0$  oscillations for the six different  $r$  intervals. The curves are the results of the fits for  $\omega_l$ .

## 5 Vertex reconstruction

The vertex positions for  $f_{tag}$  and  $f_{CP}$  decays are reconstructed using tracks that have at least one 3-dimensional coordinate determined from the hits in the SVD. Each vertex position is required to be consistent with the interaction point profile smeared in the plane perpendicular to the beam axis by the  $B$  meson decay length. The  $f_{CP}$  vertex is determined using the lepton tracks from  $J/\psi$  or

**Table 2.** The event fractions ( $f_l$ ) and incorrect flavor assignment probabilities ( $w_l$ ) for each  $r$  interval extracted from data.

| $l$ | $r$           | $f_l$             | $w_l$                     |
|-----|---------------|-------------------|---------------------------|
| 1   | 0.000 – 0.250 | $0.393 \pm 0.014$ | $0.470^{+0.031}_{-0.035}$ |
| 2   | 0.250 – 0.500 | $0.154 \pm 0.007$ | $0.336^{+0.039}_{-0.042}$ |
| 3   | 0.500 – 0.625 | $0.092 \pm 0.005$ | $0.286^{+0.037}_{-0.035}$ |
| 4   | 0.625 – 0.750 | $0.100 \pm 0.005$ | $0.210^{+0.033}_{-0.031}$ |
| 5   | 0.750 – 0.875 | $0.121 \pm 0.006$ | $0.098^{+0.028}_{-0.026}$ |
| 6   | 0.875 – 1.000 | $0.134 \pm 0.006$ | $0.020^{+0.023}_{-0.019}$ |

$\psi(2S)$  decays, or the prompt tracks from  $\eta_c$  decays. The decay vertex of the tagging  $B$  is determined from well measured tracks not assigned to  $f_{CP}$ . The vertex fitting procedure is iterative: the track with the largest contribution to the  $\chi^2$  is removed and the fit is repeated until the total  $\chi^2$  is small enough. The average  $z_{CP}$  resolution is  $75 \mu\text{m}$ , the  $z_{tag}$  resolution is  $140 \mu\text{m}$  as estimated from the Monte Carlo simulation.

The resolution function for the proper time interval is parametrized as a sum of two Gaussian components, with the second Gaussian used to describe the contribution of poorly reconstructed tracks. The relative fraction of the main Gaussian is determined to be  $0.982 \pm 0.013$  from a study of  $B^0 \rightarrow D^{*-}\ell^+\nu$  events (Fig. 5). The reliability of the resolution function parameterization is confirmed by lifetime measurements of  $B^0$  and  $B^+$  which are in good agreement with the world average values [7].

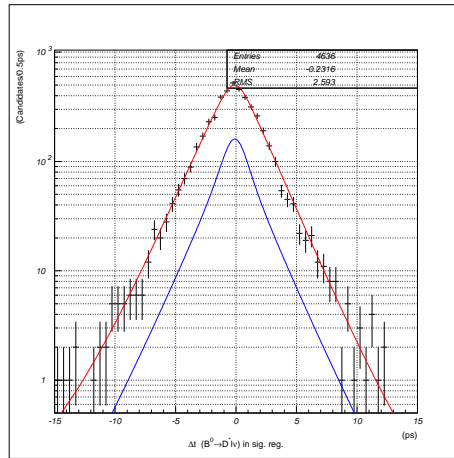


**Figure 5.** The  $\Delta t$  distribution for  $B^0 \rightarrow D^{*-}\ell^+\nu$  decays. The upper curve is the result of the fit for  $B^0$  lifetime, the lower one shows the background contribution.

## 6 $CP$ fit

We determine  $\sin 2\phi_1$  from an unbinned maximum-likelihood fit to the observed  $\Delta t$  distribution. The probability density function (pdf) expected for the signal distribution is given by

$$\mathcal{P}_{sig}(\Delta t, q, \omega_l, \xi_f) = \frac{\exp(-|\Delta t|/\tau_{B^0})}{2\tau_{B^0}} (1 - \xi_f q (1 - 2\omega_l) \sin 2\phi_1 \sin \Delta m \Delta t).$$

In this formula the  $B^0$  lifetime  $\tau_{B^0}$  and  $\Delta m$  are fixed to their world average values [7]. The pdf used for background events is

$$\mathcal{P}_{bkg}(\Delta t) = f_\tau \frac{\exp(-|\Delta t|/\tau_{bkg})}{2\tau_{bkg}} + (1 - f_\tau)\delta(\Delta t),$$

where  $f_\tau$  is the fraction of the background component with effective lifetime  $\tau_{bkg}$  and  $\delta(\Delta t)$  is the Dirac delta function.  $f_\tau$  and  $\tau_{bkg}$  are determined from the data using events in the sidebands of  $\Delta E$  vs.  $M_{bc}$  for all  $f_{CP}$  modes other than  $J/\psi K_L$ . The special treatment is performed for the  $J/\psi K_L$  background since it is dominated by  $B \rightarrow J/\psi X$  decays where some backgrounds are  $CP$  eigenstates. Fortunately this background is reliably reproduced by the Monte Carlo simulation. We use the MC background parameterization with the fraction of  $CP = +1$  and  $CP = -1$  in the  $B^0 \rightarrow J/\psi K^{*0}(K_L\pi^0)$  decay fixed from our measurements of the  $J/\psi$  polarization in  $B^0 \rightarrow J/\psi K^{*0}(K_S\pi^0)$  decay [8].

The pdfs are convolved with the vertex resolution function  $R(\Delta t)$  to determine the likelihood value for each event as a function of  $\sin 2\phi_1$ :

$$\mathcal{L}_i = \int \{f_{sig}\mathcal{P}_{sig}(\Delta t', q, w_l, \xi_f) + (1 - f_{sig})\mathcal{P}_{bkg}(\Delta t')\}R(\Delta t - \Delta t')d\Delta t',$$

where  $f_{sig}$  is the probability that the event is signal. Maximizing the total likelihood function  $L = \prod_i \mathcal{L}_i$ , where the product is over all events, we find the most probable value

$$\sin 2\phi_1 = 0.58_{-0.34-0.10}^{+0.32+0.09},$$

where the first error is statistical and the second is systematic.

Fig. 6(a) shows  $-2 \log L/L_{max}$  as a function of  $\sin 2\phi_1$  for the  $\xi_f = -1$  and  $\xi_f = +1$  modes separately and for both modes combined. Fig. 6(b) shows the asymmetry obtained by performing the fit to events in  $\Delta t$  bins separately, together with a curve representing  $\sin 2\phi_1 \sin \Delta m \Delta t$  for  $\sin 2\phi_1 = 0.58$ .

The systematic error is dominated by the uncertainties in  $\omega_l$  ( $_{-0.07}^{+0.05}$ ), and the  $J/\psi K_L$  background ( $\pm 0.05$ ). A check of the method is performed by applying the same fit to non- $CP$  eigenstate modes:  $B^0 \rightarrow D^{*-}\ell^+\nu$ ,  $D^{(*)-}\pi^+$ ,  $D^{(*)-}\rho^+$  and  $J/\psi K^{*0}(K^+\pi^-)$ , where “ $\sin 2\phi_1$ ” should be zero, and the charged  $B$  decay into  $J/\psi K^+$ . For all modes combined we find “ $\sin 2\phi_1$ ” =  $0.065 \pm 0.075$  consistent with a null asymmetry.

To conclude, we have presented a measurement of the Standard Model  $CP$  violation parameter  $\sin 2\phi_1$  based on a  $10.5 \text{ fb}^{-1}$  data sample collected at the  $\Upsilon(4S)$  resonance:

$$\sin 2\phi_1 = 0.58_{-0.34}^{+0.32}(\text{stat})_{-0.10}^{+0.09}(\text{syst}).$$

## Acknowledgments

We wish to thank the organizers of this conference for their hospitality. We also would like to acknowledge the KEKB accelerator group for the excellent operation of the collider.

## References

- [1] J.H.Christenson *et al.*, Phys. Rev. Lett. **13**, 138 (1964).
- [2] M.Kobayashi and T.Maskawa, Prog. Th. Phys. **49**, 652 (1973).

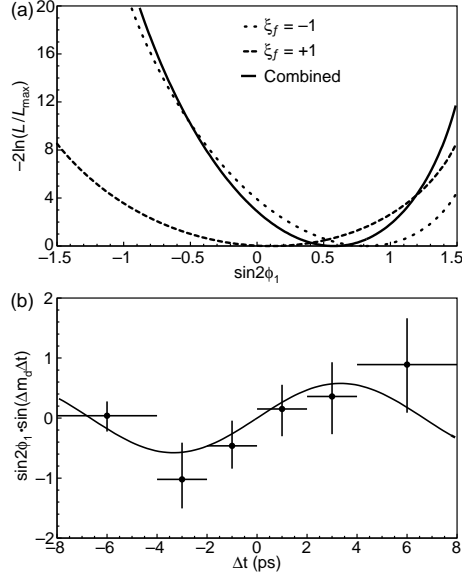


Figure 6. (a) Values of  $-2 \log L/L_{max}$  vs.  $\sin 2\phi_1$  for the  $\xi_f = -1$  and  $\xi_f = +1$  modes separately and for both modes combined. (b) The asymmetry obtained from separate fits to each  $\Delta t$  bin; the curve is the result of the global fit for  $\sin 2\phi_1 = 0.58$ .

- [3] M.Gronau and D.London, Phys. Rev. **D55**, 2845 (1997);  
R.Fleisher, *CP-Violation Beyond the Standard Model*, **CERN-TH/97-241**, Sep. 1997;  
Y.Grossman and M.P.Worah, Phys. Lett. **B395**, 241 (1997).
- [4] K.Abe *et al.* (Belle Collab.), *The Belle Detector*, KEK Report 2000-4, to appear in Nucl. Instr. and Methods.
- [5] KEKB B Factory Design Report, KEK Report 95-1, 1995, unpublished.
- [6] References in this report to a specific charged state are to be interpreted as implying the charge conjugate state also.
- [7] D.E.Groom *et al.* (Particle Data Group), Eur. Phys. J. **C15**, 1 (2000).
- [8] Belle Collab., *Measurement of polarization of  $J/\psi$  in  $B^0 \rightarrow J/\psi K^{*0}$  and  $B^+ \rightarrow J/\psi K^{*+}$  Decays*, Contributed paper (#285) to the 30<sup>th</sup> International Conference on High Energy Physics, July 2000, Osaka.